

## SURFACE DEFORMATION DUE TO COMPRESSED AIR TUNNELING USING TOUGH2 AND FLAC3D

Avirut Chinkulkijniwat

School of Civil Engineering  
Suranaree University of Technology  
Nakhon-Ratchasima 30000  
THAILAND  
e-mail: avirut@sut.ac.th

### ABSTRACT

In this study, TOUGH2-FLAC3D coupling is employed to simulate flow and deformation due to two-phase flow induced by the application of air pressure into the subsurface. Linear elastic behavior is assumed. To verify the TOUGH2-FLAC3D simulation, I use test results from an *in situ* air flow test in Essen, Germany. Comparison between calculation results and the corresponding test results showed good agreement, I carried out a simulation of compressed air tunneling, which accurately captured surface heaving in front of the tunnel face.

### INTRODUCTION

The “new Australian tunneling method” (NATM) is often used in urban tunneling (in combination with compressed air) to prevent groundwater inflow at a tunnel face. Owing to the greater magnitude of air pressure as opposed to groundwater pressure in the surrounding soil, upward air flow can predominate in the tunnel vicinity. This upward air flow can influence surface displacements during tunnel advancement.

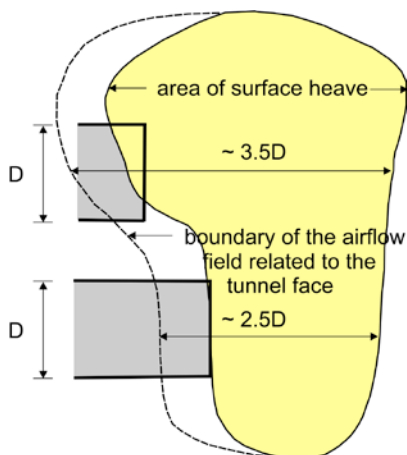


Figure 1. Inverse modeling procedures

Field observations have shown reduction in surface settlements at the tunnel tail, as well as the upward heaves at the surface ahead of the tunnel face in

compressed air tunneling—e.g., Schumacher et al. (1987), Weber (1987), and Soos and Weber (1995). Figure 1 shows a surface heaving zone observed during the subway construction in Essen, Germany (Schumacher et al., 1987). As indicated by the figure, a zone of surface heaving is created in front of the tunnel face.

Here, I focus first on the TOUGH2-FLAC3D coupling as introduced by Rutqvist et al. (2002). Then, I examine whether a loose coupling between the two codes can capture the features of flow and deformation caused by introducing air pressure into the subsoil. The results of the German field test as interpreted by Kramer & Semprich (1989) are used in this paper for this purpose. Thereafter, I conduct a simulation of compressed air tunneling, with the principal aim of checking whether the pattern of surface displacements observed in the field can be captured by considering effects of the tunnel excavation and the fluid flow. In this way, the case study is simplified by assuming a homogeneous, isotropic, and linear elastic soil domain.

### TOUGH2-FLAC3D COUPLING

The TOUGH2-FLAC3D coupling is conducted following Rutqvist et al. (2002), i.e., sequential execution and data transfer via a set of external ASCII files. TOUGH2 has been developed to handle nonisothermal, multiphase, multicomponent fluid flows in 3-dimensional porous and fracture media. However, mechanical simulation is not possible in a stand-alone TOUGH2 simulation. FLAC3D has been developed to perform mechanical simulation in soils and rocks. Although FLAC3D can also handle fluid-mechanical interactions for single-phase fluid flow, a simulation of two-phase fluid flow is not possible with a stand-alone FLAC3D simulation. Using a sequential coupling of two codes is more time consuming than using a single code. However, the big advantage of coupling TOUGH2 and FLAC3D is that both of them are used worldwide and are well tested in their respective fields. Additionally, source code is available for TOUGH2, and thus modification

of the code as well as implementation of the constitutive transport equations is possible. Moreover, in FLAC3D, an embedded programming language, the so-called FISH language, enables the user to define any new variables and functions. FLAC3D can communicate with TOUGH2 via this feature.

In order for FLAC3D and TOUGH2 to communicate with each other, knowledge of their corresponding meshes (and how the data structure is stored in the meshes) must be established. A finite difference mesh in FLAC3D generated by the user consists of elements and nodal points. An element is the smallest geometric domain within which the change in a phenomenon (e.g., stress versus strain) is evaluated. Nodal points are points at the corners of the corresponding element. In FLAC3D, state variables that are the vector quantities are stored at the nodal points, and state variables that are the scalar and tensor quantities are stored at the element centroids. However, the input variables can be submitted into the FLAC3D mesh only through the FLAC3D nodal points. The TOUGH2 mesh does not use nodal points, but rather elements. Therefore, all the state variables in TOUGH2 are stored at the element centroids.

The effective stress at each FLAC3D element is calculated from the degree of liquid saturation  $S_l$ , the pressure of liquid phase  $p_l$ , and the pressure of gas phase  $p_g$ , which are calculated in TOUGH2.

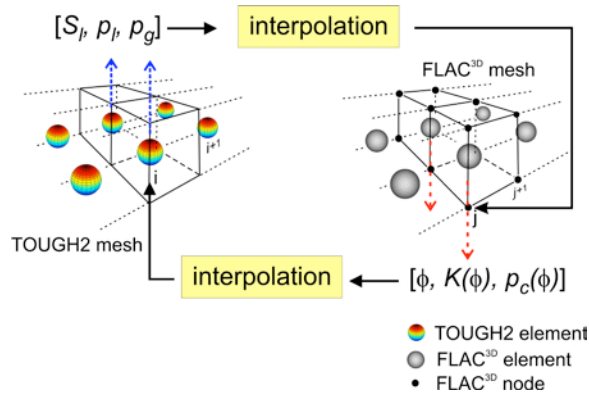


Figure 1. Communication between TOUGH2 and FLAC3D

An increment in porosity is calculated from a volumetric strain. In this paper, the volumetric strain is calculated based on an assumption of linear elastic deformation. The volumetric strain increment is stored at a FLAC3D element centroid, with an updated porosity representing the corresponding element centroid. After the FLAC3D simulation run, that updated porosity is then sent to a corresponding

TOUGH2 element. Figure 1 is schematic diagram showing how information from the TOUGH2 mesh is sent to the  $j$ th FLAC3D node and how the information from the FLAC3D mesh is sent to the  $i$ th TOUGH2 element.

The TOUGH2-FLAC3D coupling is initiated with a TOUGH2 simulation run. TOUGH2 is executed between  $t_0$  and  $t_1$  until convergence is reached. At each TOUGH2 element, porosity is assumed constant during this time step. Then, FLAC3D is executed for mechanical simulation for the same time step. The effective stress at each FLAC3D element is calculated. At the end of each time step, an increment in porosity is calculated from a volumetric strain as written in Equation 3. TOUGH2 is then executed for the next time step. The updated porosity after the FLAC3D simulation run is then sent to a corresponding TOUGH2 element. TOUGH2 is again executed between  $t_1$  and  $t_2$  until convergence is reached. These procedures are repeated until the simulation time reaches a time specified by the user. Fig. 1 shows the numerical procedures for coupling TOUGH2 and FLAC3D.

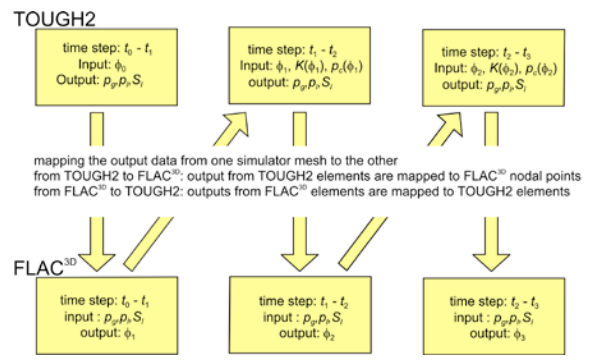


Figure 2. TOUGH2-FLAC3D coupling procedures

Between fluid flow and mechanical simulations in Figure 2, interpolation is required to map inputs and outputs from one mesh to the other—this is because the variables are submitted into FLAC3D mesh through its nodal points, while TOUGH2 mesh uses only elements. Moreover, even the outputs from FLAC3D are at FLAC3D elements. In a loose coupling of the two codes, the computational grid mesh used in each is not necessary, and therefore the same interpolation is required. In this study, a weighted distant interpolation is used for interpolation inside the domain. At the boundaries of the model, the closest point is searched and assigned to the destination, point by point.

**SIMULATION RESULTS OF AIR FLOW TEST**

The *in situ* air flow test in Essen carried out by the German contractor Bilfinger + Berger Bauaktien-

gesellschaft (Kramer & Semprich 1989) is chosen to test the coupled simulation. This air-flow test was carried out—simultaneously with a tunneling construction project in Essen, Germany—to investigate the fluid conductivity of the gas phase and the deformations due to two-phase flow induced by introducing compressed air into the subsurface. Figure 3 shows a schematic diagram of the experimental setup. Details of the experiment are elaborately discussed in English in Chinkulkijniwat et al. (2006).

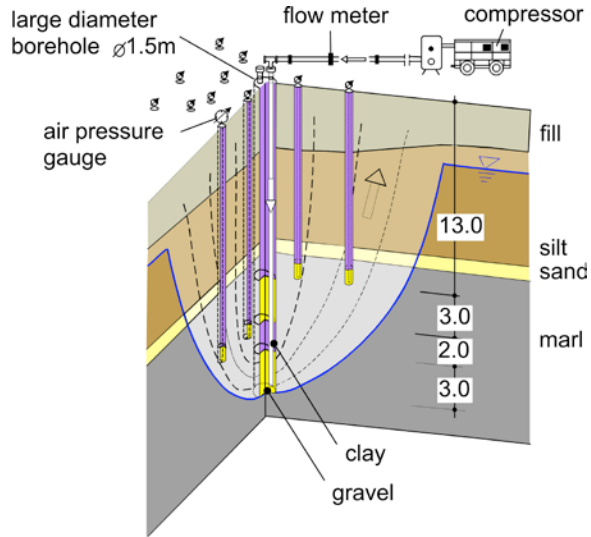


Figure 3. In situ air flow test in Essen (Kramer & Semprich, 1989)

Figure 4 shows the calculated pore pressure and gas saturation after 27 hours of air pressure injection ( $p_a = 160 \text{ kN/m}^2$ ) into the borehole. The distribution of pore pressure after 27 hours of applying that air pressure is shown in Figure 6a. The pore pressure increases significantly in the vicinity of the borehole, but retains its level of hydrostatic pressure at a certain distance apart from the borehole. The levels of pore pressure measured from 4 piezometers are also shown in Figure 4a. As can be seen in Figure 4a, good agreement between the measured and calculated pore pressures is achieved. The distribution of gas saturation after 27 hours of applying the  $160 \text{ kN/m}^2$  of air pressure into the borehole is shown in Figure 4b, with the desaturation zone in the marl layer taking on a bulb-like shape. In this marl layer, a high degree of gas saturation can be found in the vicinity of the air injection zone, but only a small area of the marl layer is desaturated. Within the sand layer, because of its relatively high fluid-conductivity value, the desaturation zone spreads over the entire layer. However, in the silt layer, the desaturation zone does not exist, due to its low fluid conductivity value and high air-entry-pressure value.

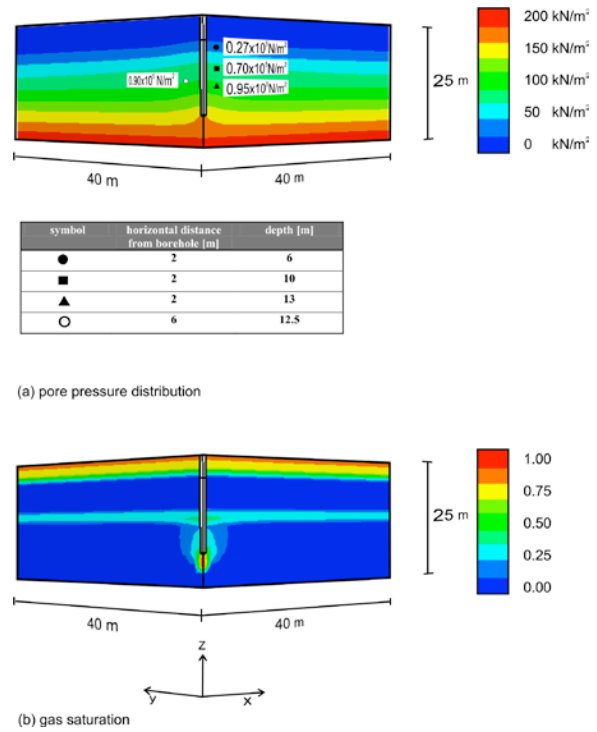


Figure 4. Pore-pressure distribution and gas saturation

Figure 5 shows a comparison between the surface displacement measured from the experiment and that calculated from the loose-coupling simulation at 27 hours, after introducing  $160 \text{ kN/m}^2$  of air pressure into the borehole. The blue diamonds are experimental results. Keeping in mind that each soil layer is assumed homogeneous and isotropic, we note the good agreement between the experimental results and the numerical results, even with the level of surface displacement in the numerical simulation being somewhat higher than that found in the experiment.

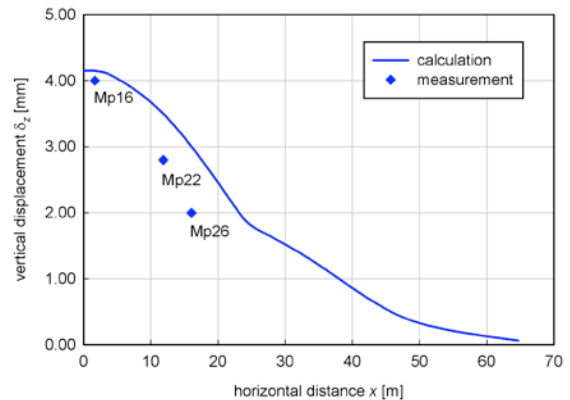


Figure 5. Surface displacement due to the first air pressure level in the test

## SIMULATION RESULTS OF COMPRESSED AIR TUNNELING

To simulate the compressed air tunneling, I assumed a silty sand layer, 20 m thick, with a bulk density of 2000 kg/m<sup>3</sup>, which converts to a dry density of 1.62 g/cm<sup>3</sup>. The silty sand layer is underlined by a thick layer of impervious bedrock, and the groundwater table is at the ground surface. A 6 m diameter circular-shaped tunnel is being excavated within these ground conditions by means of NATM using compressed air. A tunnel base is located at 15 m below the groundwater table. (Figure 6 shows these ground conditions.) According to the location of the tunnel base, air pressure in this example is about 150 kN/m<sup>2</sup>. The rate of tunnel advance is assumed to be  $v = 4$  m/day. Physical, mechanical, and fluid properties of the silty sand are summarized in Table 1 and Table 2.

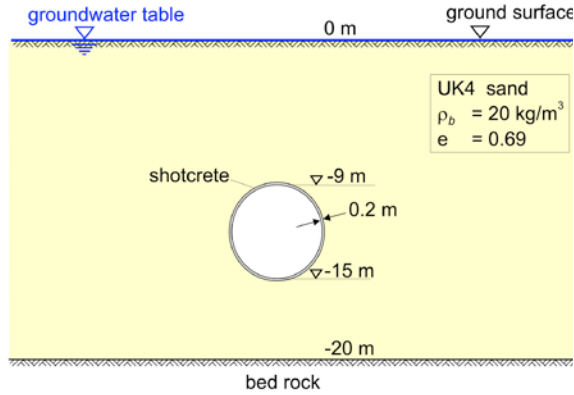


Figure 6. Ground conditions and geometry of the tunnel

Table 1. Properties of the silty sand

		Unit
Grain density	$\rho_s$	2.74 [g/cm <sup>3</sup> ]
Dry density	$\rho_d$	1.62 [g/cm <sup>3</sup> ]
Young modulus	$E$	45 [MN/m <sup>2</sup> ]
Poisson's ratio	$\nu$	0.3 [-]

Table 2. Fluid related properties of silty sand

Parameter		Unit
$K$	$1.50 \times 10^{-9} \phi^{6.4}$	[m <sup>2</sup> ]
$S_{ls}$	0.98	[-]
$n$	3.55	[-]
$S_{lr}$	0	[-]
$p_o$	6.80	[kN/m <sup>2</sup> ] <sup>-1</sup>
$\tau$	2.76	[-]

Parameters in Table 2 follow the constitutive flow equations written in Equations 1 to 3, where  $p_o$  is the air entry pressure,  $k_{rl}$  is the relative permeability of the liquid phase,  $k_{rg}$  is the relative permeability of the gas phase,  $\tau$  is the tortuosity-related parameter representing how long the liquid-flow component increases as the liquid saturation decreases,  $n$  is the pore-size distribution-related parameter,  $S_l$  is liquid saturation,  $S_{lr}$  is residual liquid saturation,  $S_{ls}$  is maximum liquid saturation, and  $\phi$  is porosity.

$$p_c = p_o ((S_e)^{-n/n-1} - 1)^{1/n} \quad (1)$$

$$k_{rl} = (S_e)^t \left[ 1 + (1 - (S_e)^{n/n-1})^{1-1/n} \right]^2 \quad (2a)$$

$$k_{rg} = (1 - S_e)^t \left[ 1 - (S_e)^{n/n-1} \right]^{2(1-1/n)} \quad (2b)$$

$$S_c = \frac{S_l - S_{lr}}{S_{ls} - S_{lr}} \quad (3)$$

Figure 7 shows simulation results of the surface deformation for the tunnel face position  $y = 40$  m. When the tunnel face is at  $y = 40$  m, cross sections of surface displacements at  $y = 10$  m,  $y = 30$  m,  $y = 40$  m, and  $y = 50$  m are shown in Fig. 7. A combination of the settlements due to excavation and the upward heaves due to seepage flow is exhibited. The most pronounced zone of upward heaves is shown within a certain distance in front of the tunnel especially along the centre line of the tunnel.

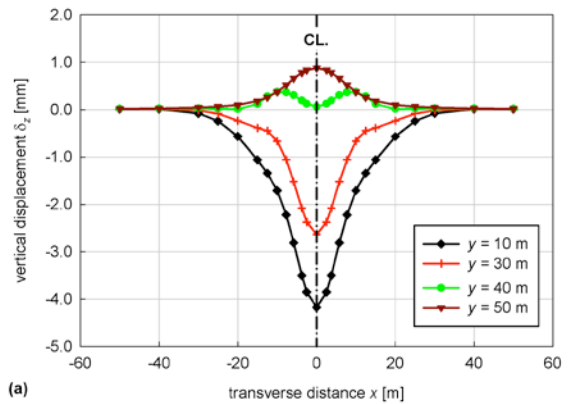


Figure 7. Surface displacements for the tunnel face at  $y = 40$  m

## **CONCLUSION**

The results from the TOUGH2-FLAC3D coupling simulation show good agreement with the corresponding test results, indicating that the TOUGH2-FLAC3D coupling can capture flow and deformation features resulting from air pressure introduced into the subsoil. The next step is to implement an elasto-plastic model for unsaturated soils into FLAC3D and extend the simulation to explain surface settlement due to compressed air tunneling construction.

## **REFERENCES**

- Chinkulkijniwat, A., Semprich, S. (2006). Flow-Deformation due to Two-Phase Flow A Loose Coupling Simulation. Proc. 6th European Conf. Numerical Methods in Geotechnical Engineering, Graz, Austria, September 6-8, 2006, 693-698.
- ITASCA Consulting Group Inc. (2002). Fast Lagrangian Analysis of Continua in 3 Dimensions Version 2.10, User's Manual. ITASCA Consulting Group Inc, Minnesota.
- Kramer, J., Semprich, S. (1989). Erfahrungen über Druckluftverbrauch bei der Spritzbetonbauweise. Taschenbuch für den Tunnelbau. 13. Jahrg, Verlag Glückauf GmbH, Essen, 91-153.
- Pruess, K., Oldenburg, C., Moridis, G. (1999). TOUGH2 User's Guide, Version 2.0. Earth Science Division, Ernest Orlando Lawrence Berkeley National Laboratory.
- Rutqvist, J., Wu, Y. -S., Tsang, C.F., Bodvarsson, G. (2002). A modeling approach for analysis of coupled multiphase fluid flow, heat transfer, and deformation in fractured porous rock. Int. J. of Rock Mechanics & Mining Sciences, Vol. 39, 429-442.
- Schumacher, G., Haardt, H., Kalthoff, D. (1987). U-Bahn Bau in Essen, Baulos 30, Spritzbetonbauweise unter Druckluft – Baukonzept und Bauarwicklung. Forschung und Praxis, Vol. 32, 184-192.
- Soos, P.v., Weber, J. (1995). Druckluftvortriebe im Münchner U-Bahn-Bau. Schriftenreihe Lehrstuhl und Prüfamnt für Grundbau. Bodenmechanik und Felsmechanik der TU München, Germany, Heft 21, 261-279.
- Weber, J (1983). Erfahrungen mit Druckluftvortrieben in Spritzbetonbauweise beim Mühener U-Bahn-Bau, STUVA Tagung 1983 in Nürnberg. Forschung und Praxis, Vol. 32, 184-192.